Atmos. Chem. Phys. Discuss., 10, 21023–21046, 2010
www.atmos-chem-phys-discuss.net/10/21023/2010/
doi:10.5194/acpd-10-21023-2010

Atmospheric Chemistry and Physics Discussions

Total cloud cover from satellite observations and climate models

P. Probst[1], **R. Rizzi**[1], **E. Tosi**[1], **V. Lucarini**[1,2,3], **and T. Maestri**[1]

[1]Department of Physics, University of Bologna, Bologna, Italy
[2]Department of Meteorology, University of Reading, Reading, UK
[3]Department of Mathematics, University of Reading, Reading, UK

Received: 17 August 2010 – Accepted: 23 August 2010 – Published: 2 September 2010

Correspondence to: R. Rizzi (rolando.rizzi@unibo.it)

Published by Copernicus Publications on behalf of the European Geosciences Union.

Abstract

Global and zonal monthly means of cloud cover fraction for *total* cloudiness (CF) from the ISCCP D2 dataset are compared to same quantity produced by the 20th century simulations of 21 climate models from the World Climate Research Programme's (WCRP's) Coupled Model Intercomparison Project phase 3 (CMIP3) multi-model dataset archived by the Program for Climate Model Diagnosis and Intercomparison (PCMDI). The comparison spans the time frame from January 1984 to December 1999 and the global and zonal average of CF are studied. The restriction to total cloudiness depends on the output of some models that does not include the 3D cloud structure. It is shown that the global mean of CF for the PCMDI/CMIP3 models, averaged over the whole period, exhibits a considerable variance and generally underestimates the ISCCP value. Very large discrepancies among models, and between models and observations, are found in the polar areas, where both models and satellite observations are less reliable, and especially near Antarctica. For this reason the zonal analysis is focused over the 60° S–60° N latitudinal belt, which includes the tropical area and mid latitudes. The two hemispheres are analyzed separately to show the variation of the amplitude of the seasonal cycle. Most models overestimate the yearly averaged values of CF over all of the analysed areas, while differences emerge in their ability to capture the amplitude of the seasonal cycle. The models represent, in a qualitatively correct way, the magnitude and the weak sign of the seasonal cycle over the whole geographical domain, but overestimate the strength of the signal in the tropical areas and at mid-latitudes, when taken separately. The interannual variability of the two yearly averages and of the amplitude of the seasonal cycle is greatly underestimated by all models in each area analysed. This work shows that the climate models have an heterogeneous behaviour in simulating the CF over different areas of the Globe, with a very wide span both with observed CF and among themselves. Some models agree quite well with the observations in one or more of the metrics employed in this analysis, but not a single model has a statistically significant agreement with the observational datasets

ACPD

10, 21023–21046, 2010

on yearly averaged values of CF and on the amplitude of the seasonal cycle over all analysed areas.

1 Introduction

Clouds constitute one of the major factors in determining the Earth radiation budget. They profoundly influence the general circulation of the atmosphere, the hydrological cycle and the atmospheric and surface energy budget. Many studies show the crucial role of clouds in modulating the climate (e.g., Stephens et al., 1990; Poetzsch-Heffter et al., 1995; Senior, 1999; Yao and Del Genio, 1999; Liou, 2002; Cess and Udelhofen, 2003; Williams et al. , 2006; IPCC, 2007). Small changes in the location or frequency of clouds can impact the climate in a very substantial way. Moreover, improvements in the representation of clouds constitute a crucial goal for climate modellers, since the uncertainty about the intensity of the clouds feedback on climate is considered as the major obstacle to improving the climate change predictions (IPCC, 2007). The scientific debate concerning the strategies to achieve efficient and accurate parameterizations for clouds in climate models is very intense (e.g., Arking, 1991; Ridout and Rosmond, 1996; Webb et al., 2001; Weare, 2004; Schmidt et al., 2006; Stowasser and Hamilton, 2006; Su et al., 2006; Tsushima et al., 2006; Reichler and Kim, 2008; Vavrus et al., 2008; Wilkinson et al., 2008; Woods et al., 2008; Waliser et al., 2009). In particular Arking (1991) shows how ice and liquid clouds are often poorly represented in general circulation models; Waliser et al. (2009) show that the accurate representation of tropospheric ice clouds is a difficult goal for the model development community while Vavrus et al. (2008) show the difficulties of the climate models in simulating the Arctic cloud cover.

A recent study by Pincus et al. (2008) describes a method for evaluating the performance of climate models by comparing the simulation of the present-day distribution of clouds, radiation and precipitation, to global observations. The satellite observational data, processed into a cloud climatology, are in fact essential both to improve the cloud model parameterizations and also to verify their quality in reproducing cloudiness.

Several remote sensing techniques are used to detect and distinguish cloud types. These procedures involve the interpretation and inversion of electromagnetic radiation measured by satellite radiometers (Kidder and Haar, 1995). The present work considers one of the products of the International Satellite Cloud Climatology Project (ISCCP), the D2 dataset (Rossow et al., 1987) which provides monthly values of several variables. This dataset is used to evaluate the performance in simulating the cloud coverage of 21 climate models whose comprehensive outputs were collected and stored by the Program for Climate Model Diagnosis and Intercomparison (PCMDI) in the World Climate Research Programme's (WCRP's) Coupled Model Intercomparison Project phase 3 (CMIP3) multi-model dataset, a project of the US Lawrence Livermore National Laboratory. Henceforth the considered climate models are denoted as PCMDI/CMIP3 models. It is important to highlight that the PCMDI/CMIP3 dataset has played a vital role for the scientific research which has lead to the preparation of the IPCC Fourth Assessment Report (IPCC4AR). Since the clouds vertical structure is not available in the output files for most PCMDI/CMIP3 models, our analysis is confined to the cloud cover fraction of *total* cloudiness (CF), and compares the CF monthly mean from the ISCCP D2 dataset with same quantity from the PCMDI/CMIP3 models listed in Table 1, for the common time frame from January 1984 to December 1999.

In Sect. 2 a brief description of observational and model data used in this analysis is presented. The most important results stemming from the comparison are discussed in Sect. 3, while the concluding remarks are drawn in Sect. 4.

2 Observational and model data

The International Satellite Cloud Climatology Project (ISCCP) is the first project of the World Climate Research Program (WCRP) in order to study the role of clouds in the Earth radiation budget and in the hydrological cycle. Since July 1983 the visible (0.6 µm) and infrared (11 µm) radiances, measured by imaging radiometers carried

ACPD
10, 21023–21046, 2010

on polar and geostationary satellites, have been collected and processed into a cloud climatology. A detailed description of the methodology is given in Rossow and Garder (1993a).

Many ISCCP datasets are available on the ISCCP web site, with several temporal and spatial resolutions. In this study we consider the CF monthly means on an Equal-Area Grid ($280\times280\,km^2$), which are part of the D2 dataset. More information can be found in Rossow et al. (1987); Rossow and Shiffer (1991); Rossow and Garder (1993b); Rossow et al. (1993, 1996); Rossow and Shiffer (1999); Rossow and Duenas (2004); ISCCP web site. The ISCCP D2 Data Set is the best known and most widely used cloud dataset, although it must be used with great care as many unphysical factors may act together to determine spurious statistical properties for the CF. One of the most important problems is the detection of multi-layer clouds, since only the uppermost cloud layer at each location can be observed. Another common limitation when using the satellite observations is the drift in the Equatorial Crossing Time (ECT) over the life span of a polar satellite and the possibly correlated trend of cloud cover. The shift in ECT has some implications both on the calibration of the satellite instruments over time and on the combined use of data from different satellites for meteorological analysis. It is however crucial in the definition of a climatologically-relevant dataset (Stowe et al., 2002). Another limit of the ISCCP cloud detection algorithm is the low efficiency in identifying the presence of clouds over iced surfaces. Recent studies have also shown that some CF trends can be explained by factors other than physical changes occurring in the atmosphere. For example, the number of geostationary satellites available varies in time and consequently the average view angle changes as the dataset is being accumulated thus creating a viewing geometry artifact (Campbell, 2004, 2006). Moreover, the switch to the new generation of Advanced Very High Resolution Radiometer (AVHRR), when the NOAA-16 replaced NOAA-14, has introduced a shift, during the 2001–2002 period (Evan et al., 2007) and the definition of an agreed procedure for taking care of this last issue is still not conclusive.

ACPD
10, 21023–21046, 2010

Title Page
Abstract | Introduction
Conclusions | References
Tables | Figures
◀◀ | ▶▶
◀ | ▶
Back | Close
Full Screen / Esc
Printer-friendly Version
Interactive Discussion

The Coupled Model Intercomparison Project (CMIP), established by the Working Group on Coupled Modelling (WGCM) under the WCRP, is a standard experimental protocol to study the coupled atmosphere-ocean general circulation models. These models are designed to simulate the climate variability and the climate response to forcings, such as changes in solar irradiance and in atmospheric CO_2 concentration. The third phase of this experiment (CMIP3) included the "realistic" scenarios for both past and present climate forcing, therefore the CMIP3 multi-model dataset contains several simulations, including the reconstruction of the past and present climate and the future climate projections (see on PCMDI web site the complete experiments list).

The experiment considered in this work is that aimed at representing the 20th Century Climate. It describes the evolution of climate from the industrial revolution ($\simeq$ 1850) to 2000, by specifying the observed concentrations of greenhouse gas (e.g. CO_2, CH_4, N_2O, CFCs) and, for some models, by including also the following forcing agents: natural and anthropogenic sulfate aerosols, volcanic activity and solar irradiance variations. In Table 1 only the latter forcing is shown, while all the forcing agents are documented on PCMDI web site. For each model, the 20th Century simulation starts from initial conditions provided by the pre-industrial control run, where an (approximate) steady state is obtained as a result of a long integration performed with fixed atmospheric composition (most notably, the CO_2 concentration is set to 280 ppm). See PCMDI web site and Meehl et al. (2007) for more information.

In the present work the CF monthly averages for the period January 1984–December 1999 are considered as the metric for auditing the PCMDI/CMIP3 models (Lucarini, 2008).

3 Cloud fraction comparisons between ISCCP D2 data and PCMDI/CMIP3 model runs

In Fig. 1 the CF global monthly mean values, averaged over the whole period under study (Jan 1984-Dec 1999), are shown for all models. Very different values in the total

ACPD
10, 21023–21046, 2010

global mean CF are observed in the models ensemble: most models underestimate the ISCCP value (bold blue line), except the CNRM-CM3 model, which overestimates the value. Typically, the models feature a remarkable negative bias of the order of 10–15%.

In order to explore the reasons for such a large global bias, we study how the climate models represent the zonal variations of the CF. The CF zonal mean, averaged over the whole period, of the ISCCP D2 dataset and of the PCMDI/CMIP3 models is shown versus latitude in Fig. 2. The models ensemble mean of the CF zonal profile (*PCMDI/CMIP3 mean model*) is portrayed in Fig. 3 with the standard deviation of the models' mean. Such a figure has been constructed by remapping the models zonal profiles to a common resolution (see Table 1 for the horizontal resolution of the individual models). In same figure also the ISCCP D2 zonal mean is shown. We remark that, as discussed in Lucarini (2008), the ensemble mean and ensemble spread must be interpreted only as a qualitative representation of the typical output given by models and of their typical degree of agreement. In fact, ensemble mean and spread cannot be given any quantitative probabilistic meaning, since they are not produced as observables of a well-defined probability space.

Both figures show that nearly all models, while providing a qualitatively correct picture of the latitudinal dependence of cloud cover, underestimate the average CF for a large portion of the latitudinal belt between 60° S and 60° N, to such an extent that the ISCCP values is, in most latitudes, higher than the multi-model ensemble mean by over one multi-model ensemble standard deviation. Note that this is the latitudinal belt where observational data are most reliable. The models show a relatively better agreement with the satellite observations in the tropical area, possibly because the model tuning of the cloud and rain parametrizations are done on this area. The largest biases are found in the mid-latitudes, which points at deficiencies in the representation of mid-latitude cyclones (Lucarini et al., 2007). In terms of consistency in the models outputs, large discrepancies are found for all latitudes, with models span being 40% in the equatorial region, and consistently above 30% poleward of 50°in both hemispheres. In the

ACPD
10, 21023–21046, 2010

polar regions, in agreement with the observed difficulties in the representation of Polar clouds (Vavrus et al., 2008), the discrepancies found are of the order of 60% in the Noth Pole, whereas over Antarctica the spread of models output reaches a staggering 90%.

In order to show more precisely the degree of realism and self-consistency of the models, the yearly time average CF (spatially averaged) and the amplitude of seasonal cycle, are analysed for the 60° S–60° N latitudinal belt, where observations are more reliable and models are expected to perform better. The two hemispheres (denoted by NH and SH) are analyzed separately to show the variation of the amplitude of the seasonal cycle. Moreover, the shape of the zonal mean (see Fig. 3) suggests to analyze separately the tropical areas (0–30° N and 30–0° S) and the mid-latitudes (30–60° N and 60–30° S). Results of this concise comparison are presented in Fig. 4 for the area 60° S–60° N, in Fig. 5a and 5b for the two hemispheres, in Fig. 6a and 6b for the tropical areas and in Fig. 7a and 7b for the mid-latitudes.

Consistently with what observed in Figs. 1–3, Fig. 4 shows that all models, except CNRM-CM3, underestimate the yearly average CF, with biases up to 20%, and poor consistency within the ensamble. Since we are integrating over a symmetric latitudinal belt, we expect a weak seasonal signal, representing the asymmetry of climate in the two hemispheres. Observations feature a weak seasonal cycle signal (about 1%) with a positive value, meaning that the winter cloud coverage is larger than the summer one. For all models the CF features a weak seasonal cycle with intensity smaller than 5%, and most models capture the correct phase. Only two models – CSIRO-Mk3.0 and FGOALSg1.0 – feature statistical properties consistent with those of the observations. Interestingly, all models seriously underestimate the interannual variability of the yearly average and many underestimate the amplitude of the seasonal cycle.

When separating the two hemispheres – see Fig. 5 – all models, except CNRM-CM3 and FGOALS-g1.0 (only in NH), seriously underestimate the yearly average CF. The amplitude of the seasonal cycle for the observations and for most models has typically opposite sign in the two hemispheres, negative in the NH and positive in the SH. Note

ACPD
10, 21023–21046, 2010

that, whereas most models feature a reasonably good agreement with observations on the intensity of the seasonal cycle in the SH, the situation is less clear in the NH, where the model spread is much higher, with few models even featuring a sign opposite to that of observations. In both areas the interannual variability of the yearly average and of the seasonal cycle is underestimated in all cases. The only model in agreement with the observation in both hemispheres is CSIRO-Mk3.0. In order to gain a better understanding of such issues in the performance of the models, it is crucial to separate the CF in the tropical area and at midlatitudes, since different dominant mechanisms lead to the formation of clouds in the two areas, tropical convection and baroclinic instability, respectively.

Figures 6a and 6b suggest that, when yearly averages are considered, each model features similar average values of CF on the two sides of the equator, in agreement with the observations. All models except CNRM-CM3, CSIRO-Mk3.0, and FGOALSg1.0 consistently underestimate the average CF. Since the Intertropical Convergence Zone (ITCZ) shifts latitudinally toward the summer regions, thus moving towards north in JJA and towards south in DJF, a strong seasonal cycle of opposite sign is expected when the tropical regions of the two hemispheres are considered separately. This is a clear feature that all models capture at least in qualitative terms, even if the strength of the seasonal signal ranges, among models, between about 5% to about 20% in both hemispheres. The amplitude of the seasonal cycle is similar in both hemispheres for most models, in agreement with observations, where such amplitude is found to be of about 7%. Overall, three models – CSIRO-Mk3.0, CSIRO-Mk3.5 and GFDL2.0 – feature statistical properties compatible with those of the ISSCP dataset in both tropical regions.

Considering the mid-latitudes (Fig. 7), the yearly averaged CF is higher in the SH by 5–10% for nearly all models and for the observations. A likely reason is that the land surface fraction is much lower in the SH, so that the processes of exchange of water vapour between the atmosphere and the underlying surface are more efficient, considering that surface winds are also stronger. In both hemispheres, most models underestimate the D2 yearly averaged CF by a large amount, ranging between 10 and 20%, with larger biases observed in the SH.

For both observations and models in the NH the seasonal cycle has opposite sign (and comparable size) to the nearby tropical region. In fact, mid-latitude clouds are more abundant in the cold season since the main mechanism leading to their formation, baroclinic cyclogenesis, is stronger in the winter as the temperature difference between tropical and polar regions is higher. This physical argument holds also in the SH, where nevertheless the seasonal cycle is much weaker than its NH counterpart for all models, whereas no seasonal cycle at all is found in the observations. The weaker seasonal signal of the southern temperature difference between high and low latitudes surely plays a role in explaining this. Analogously to what observed in the tropical regions, the models typically overestimate the seasonal cycle of the mid-latitude CF in both hemispheres by a value of the order of 5–10%. Overall, for no models the statistical properties of the mid-latitudes CF are compatible with those of observations, and the degree of mutual consistency of the models is rather poor. We observe however that the model CNRM-CM3 is the closest to ISCCP data and clearly outperforms all the others in terms of realism.

4 Conclusions

In this paper the monthly mean of total cloud cover fraction (CF) is chosen as benchmark for intercomparing and validating climate models included in the PCMDI/CMIP3 project, which have contributed decisively to the IPCCAR4. The statistical properties of clouds play a decisive role in the earth climate, by providing a first order contribution to the energy budget at the top of the atmosphere (IPCC, 2007). As observational counterpart, the satellite observations of clouds constituting the ISCCP D2 dataset for the 1984–1999 time frame, are considered. These data are compared to the corresponding period of the standard 20th century simulations of 21 climate models.

ACPD
10, 21023–21046, 2010

Our results highlight that a correct representation of the statistical properties of clouds in state-of-the-art climate models is still a long way to go, as relevant systematic errors are present for basically all models in both tropical and extratropical regions. On the other hand it is also important to consider that the observational data used in this work could be affected by some possible errors, due to some problems (e.g. presence of multi-layered cloud system) and limits (e.g. ECT drift) of satellite observations and also due to a viewing geometry artifact, as recently studies (Campbell, 2004, 2006; Evan et al., 2007) have shown.

Considering the statistical properties of the annual and global averaged CF, the inter-model discrepancies found are rather large, with a range of results going from about 52% to 72%. Typically, the climate models seriously underestimate the global CF by about 10%. Moreover, models consistently underestimate the CF over almost all zonal bands. Looking at zonal averages, we also discover that the largest discrepancies among models are to be found in the tropical region and in the two polar regions, where the range of models' outputs reaches the staggering value of 40%(Tropics), 60% (North Pole) and 90% (South Pole).

Our analysis has then focused in the latitudinal band 60° S–60° N, which covers over 85% of the planet's surface, since this is the regions where both the satellite observations and model simulations are most reliable. The yearly average of the CF and its seasonal cycle, measured by the difference between the DJF and the JJA averages, are considered. In the whole latitudinal band, the models show poor consistency with each other and most of them underestimate the observative values by up to 20%, whereas most model capture in a qualitatively correct way the magnitude and the (obviously weak) sign of the seasonal cycle. When the NH band (0°–60° N) and its SH counterpart (60° S–0°) are considered separately, most models underestimate the yearly average CF in both hemispheres and the amplitude of seasonal cycle. The quality of the models output seems to be lower in the NH, where the models' bias is higher and the seasonal signal of some models is opposite to that of observations. This is probably related to difficulties in representing correctly the seasonal variations of the

ACPD
10, 21023–21046, 2010

hydrological cycle when large fraction of land-covered areas are considered (Lucarini et al., 2008).

The analysis of the tropical areas shows that the large majority of models underestimates the yearly averaged CF and overestimate its seasonal cycle in both hemispheres. This points at problems in the representation of the mean state and of ITCZ variability. Since typically the mean state of models is biased negatively by 10–15% and the amplitude is typically larger by about 5%, this means that (local) winter values (where minima are observed) are biased by more than 20–25%, whereas the (local) summer discrepancies are smaller.

When considering the mid-latitudes, a similar picture is found, with models typically largely underestimating the yearly values of CF and overestimating the amplitude of the seasonal cycle (which has opposite phase with respect to the tropical region and is stronger in the NH). This points out at deficiencies in the representation of the cyclonic activity at mid-latitude, which is mainly responsible for determining the cloud cover. Previous analyses had pointed in this direction using estimators of the atmospheric variability (Lucarini et al., 2007).

While some models agree quite well with the observations in one or more of the metrics employed in this analysis, not a single model shows a statistically significant agreement with the observational dataset of yearly averaged values of CF and on the amplitude of the seasonal cycle on both tropical and extratropical regions. Also, the span of model results is very wide, which suggest that large inter-model discrepancies are present. In spite of this "generous" inter-model uncertainty, if an ensemble model mean and variability is heuristically constructed (we have reported elsewhere that this construction, even if very used, is not really well defined (Lucarini, 2008)), the observational data are more than one standard deviation out of the ensemble mean for most of our estimators. Additionally, if one looks at higher order statistics, it is discovered that the interrannual variability of the considered estimators are greatly underestimated in all models with respect to observations.

ACPD
10, 21023–21046, 2010

This work is an attempt to stimulate further research in the field as a support to models' development. Obviously, the comparison of only a single parameter is merely the first step of our analysis which aims to clarify the accuracy of climate models in simulating clouds. A comparison accounting for the various cloud types (*high*, *middle* and *low*), being the net radiative properties of a cloud mainly dependent on its altitude, and for their integrated water and ice amounts, and with another satellite dataset are the next steps. Further investigation will be directed at understanding the properties of clouds in the next generation of climate models, whose data will soon be released by the PCMDI/CMIP5 project and will contribute to the next IPCC report.

Acknowledgements. We acknowledge the modeling groups, the Program for Climate Model Diagnosis and Intercomparison (PCMDI) and the WCRP's Working Group on Coupled Modelling (WGCM) for their roles in making available the WCRP CMIP3 multi-model dataset. Support of this dataset is provided by the Office of Science, U.S. Department of Energy. VL acknowledges the financial support of the EU-ERC project NAMASTE.

References

Arking, A.: The radiative effects of clouds and their impact on climate, Bull. Amer. Meteorol. Soc., 72, 795–813, 1991. 21025

Campbell, G. G.: View angle dependence of cloudiness and the trend in ISCCP cloudiness, 13th AMS Conference On Satellite Meteorology And Oceanography, Norfolk, VA, 9/20/2004-9/23/2004, 2004. 21027, 21033

Campbell, G. G.: Diurnal and angular variability of cloud detection: consistency between polar and geosynchronous ISCCP products, Preprints, 14th Conference on Satellite Meteorology and Oceanography, Atlanta, GA, Am. Meteor. Soc., 6.2., 2006. 21027, 21033

Cess, R. D. and Udelhofen, P. M.: Climate change during 1985–1999: Cloud interactions determined from satellite measurements, Geophys. Res. Lett., 30(1), 1019, doi:10.1029/2002GL016128, 2003. 21025

Evan, A. T., Heidinger, A. K., and Vimont, D. J.: Arguments against a physical long-term trend in global ISCCP cloud amounts, Geophys. Res. Lett., 34, L04701, doi:10.1029/2006GL028083, 2007. 21027, 21033

IPCC, Intergovernmental Panel on Climate Change: IPCC Fourth Assessment Report, Climate Change 2007, UNEP/WMO, 2007. 21025, 21032

ISCCP web site: available at: http://isccp.giss.nasa.gov. 21027

Kidder, S. Q., and Vonder Haar, T. H.: Satellite meteorology: An introduction, Academic Press, 4666 pp., 1995. 21026

Liou, K. N: An introduction to atmospheric radiation, Academic Press, California, USA, 583 pp., 2002. 21025

Lucarini, V., Calmanti, S., Dell'Aquila, A., Ruti, P. M., and Speranza, A: Intercomparison of the northern hemisphere winter mid-latitude atmospheric variability of the IPCC models, Clim. Dynam., 28(7), 829–848, 2007. 21029, 21034

Lucarini, V.: Validation of Climate Models, in Encyclopedia of Global Warming and Climate Change, edited by: Philander, G., SAGE (Thousand Oaks, USA), 1053–1057, 2008. 21028, 21029, 21034

Lucarini, V., Danihlik, R., Kriegerova, I., and Speranza, A.: Hydrological cycle in the Danube basin in present-day and XXII century simulations by IPCCAR4 global climate models, J. Geophys. Res., 113, D09107, doi:10.1029/2007JD009167, 2008. 21034

Meehl, G. A., Covey, C., Delworth, T., Latif, M., McAvaney, B., Mitchell, J. F. B., Stouffer, R. J., and Taylor, K. E.: The WCRP CMIP3 multimodel dataset, B. Am. Meteorol. Soc., 88, 1383–1394, 2007. 21028

PCMDI web site: available at: http://www-pcmdi.llnl.gov, last access: 2010. 21028

Pincus, R., Batstone, C. P., Hofmann, R. J. P., Taylor, K. E., and Glecker, P. J.: Evaluating the present-day simulation of clouds, precipitation, and radiation in climate models, J. Geophys. Res., 113, D14209, doi:10.1029/2007JD009334, 2008. 21025

Poetzsch-Heffter, C., Liu, Q., Ruperecht, E., and Simmer, C.: Effect of cloud types on the earth radiation budget calculated with the ISCCP CI dataset: Methodology and initial results, J. Clim., 8(4), 829–843, 1995. 21025

Reichler, T. and Kim, J.: How Well Do Coupled Models Simulate Today's Climate?, Bull. Am. Meteorol. Soc., 89(3), 303–311, 2008. 21025

Ridout, J. A. and Rosmond, T. E.: Global modeling of cloud radiative effects using ISCCP cloud data, J. Clim., 9(7), 1479–1496, 1996. 21025

Rossow, W. B., Kinsella, E., Wolf, A., and Garder, L. C.: International Satellite Cloud Climatology Project (ISCCP) description of reduced resolution radiance data. WMO/TD, 58, 163 pp., 1987. 21026, 21027

ACPD
10, 21023–21046, 2010

Cloud cover comparison

P. Probst et al.

Rossow, W. B.and Schiffer, R. A.: ISCCP cloud data products, Bull. Am. Meteorol. Soc., 72(1), 2–20, 1991. 21027
Rossow, W. B. and Garder, L. C.: Cloud detection using satellite measurements of infrared and visible radiances for ISCCP, J. Clim., 6(12), 2341–2369, 1993a. 21027
Rossow, W. B. and Garder, L. C.: Validation of ISCCP cloud detections, J. Clim., 6(12), 2370–2393, 1993b. 21027
Rossow, W. B., Walker, A. W., and Garder, L. C.: Comparison of ISCCP and other cloud amounts, J. Clim., 6(12), 2394–2418, 1993. 21027
Rossow, W. B., Walker, A. W., Beuschel, D. E., and Roiter, M. D.: International Satellite Cloud Climatology Project (ISCCP) Documentation of New Cloud Datasets, WMO/TD.-No, 737, 115 pp., 1996. 21027
Rossow, W. B. and Schiffer, R. A.: Advances in understanding clouds from ISCCP, Bull. Am. Meteorol. Soc., 80(11), 2261–2287, 1999. 21027
Rossow, W. B. and Duenas, E. N.: The International Satellite Cloud Climatology Project (ISCCP) web site, Bull. Amer. Meteor. Soc, 85, 167–172, 2004. 21027
Schmidt, G. A., Ruedy, R., Hansen, J. E., Aleinov, I., Bell, N., Bauer, M., Bauer, S., Cairns, B., Canuto, V., and Cheng, Y.: Present-day atmospheric simulations using GISS ModelE: Comparison to in situ, satellite, and reanalysis data, J. Clim., 19(2), 153–192, 2006. 21025
Senior, C. A.: Comparison of mechanisms of cloud-climate feedbacks in GCMs, J. Climate, 12, 1480–1489, 1999. 21025
Stephens, G. L., Tsay, S. C., Stackhouse Jr, P. W., and Flatau, P.: The relevance of the microphysical and radiative properties of cirrus clouds to climate and climate feedback, J. Atmos. Sci., 47, 1742–1753, 1990. 21025
Stowe, L. L., Jacobowitz, H., Ohring, G., Knapp, K. R., and Nalli, N. R.: The advanced very high resolution radiometer (AVHRR) Pathfinder atmosphere (PATMOS) climate dataset: Initial analyses and evaluations, J. Clim., 15(11),1243–1260, 2002. 21027
Stowasser, M. and Hamilton, K.: Relationship between shortwave cloud radiative forcing and local meteorological variables compared in observations and several global climate models, J. Clim., 19(17), 4344–4359, 2006. 21025
Su, H., Waliser, D. E., Jiang, J. H., Li, J., Read, W. G., Waters, J. W., and Tompkins, A. M.: Relationships of upper tropospheric water vapor, clouds and SST: MLS observations, ECMWF analyses and GCM simulations, Geophys. Res. Lett., 33, L22802, doi:10.1029/2006GL027582, 2006. 21025

ACPD
10, 21023–21046, 2010

Tsushima, Y., Emori, S., Ogura, T., Kimoto, M., Webb, M. J., Williams, K. D., Ringer, M. A., Soden, B. J., Li, B., and Andronova, N.: Importance of the mixed-phase cloud distribution in the control climate for assessing the response of clouds to carbon dioxide increase: a multi-model study, Clim. Dynam., 27(2), 113–126, 2006. 21025

Vavrus, S., Waliser, D., Schweiger, A., and Francis, J.: Simulations of 20th and 21st centery Arctic cloud amount in the global climate models assessed in the IPCC AR4, Clim. Dyn., 33(7–8), 1099–1115, 2008. 21025, 21030

Waliser, D. E., Li, J. F., Woods, C. P., Austin, R. T., Bacmeister, J., Chern, J., Del Genio, A., Jiang, J. H., Kuang, Z., Meng, H., Minnis, P., Platnick, S., B. Rossow, W. B., Stephens, G. L., Sun-Mack, S., Tao, W, Tompkins, A. M., Vane, D. G., Walker, C, and Wu, D. Cloud ice: A climate model challenge with signs and expectations of progress, J. Geophys. Res., 114, D00A21, doi:10.1029/2008JD010015, 2009. 21025

Weare, B. C.: A comparison of AMIP II model cloud layer properties with ISCCP D2 estimates. Clim. Dynam., 22(2), 281–292, 2004. 21025

Webb, M., Senior, C., Bony, S., and Morcrette, J. J.: Combining ERBE and ISCCP data to assess clouds in the Hadley Centre, ECMWF and LMD atmospheric climate models, Clim. Dynam., 17(12), 905–922, 2001. 21025

Wilkinson, J. M., Hogan, R. J., Illingworth, A. J., and Benedetti, A.: Use of a lidar forward model for global comparisons of cloud fraction between the ICESat lidar and the ECMWF model, Mon. Weather Rev., 136(10), 3742–3759, 2008. 21025

Williams, K. D., Ringer, M. A., Senior, C. A., Webb, M. J., McAvaney, B. J., Andronova, N., Bony, S., Dufresne, J. L., Emori, S., and Gudgel, R.: Evaluation of a component of the cloud response to climate change in an intercomparison of climate models, Clim. Dynam., 26(2), 145–165, 2006. 21025

Woods, C. P., Waliser, D. E., Li, J.-L., Austin, R. T., Stephens, G. L., and Vane, D. G.: Evaluating CloudSat ice water content retrievals using a cloud-resolving model: Sensitivities to frozen particle properties, J. Geophys. Res., 113, D00A11, doi:10.1029/2008JD009941, 2008. 21025

Wylie, D. P., Menzel, W. P., Woolf, H. M., and Strabala, K. I.: Four years of global cirrus cloud statistics using HIRS, J. Clim., 7(12), 1972–1986, 1994.

Yao, M. S.and Del Genio, A. D.: Effects of cloud parameterization on the simulation of climate changes in the GISS GCM. J. Clim., 12, 761–779, 1999. 21025

Table 1: List of PCMDI/CMIP3 models used in this study. The third column represents their horizontal and vertical resolution: the former is expressed as degrees latitude by longitude or as a triangular spectral truncation (T), and the latter is the number of vertical levels (L). The fourth column specifies models with a 3D cloud output. The last column provides an indication of the type of solar forcing used by each model.

CMIP3 I.D.	Originating Group(s)	Atmospheric Resolution	3-D Output	Solar forcing
CCSM3.0	NCAR (USA)	T85 (L26)	Yes	Variable
CGCM3.1(T63)	CCCma (CANADA)	T63 (L31)	Yes	Constant
CNRM-CM3	Météo France (FRANCE)	T42 (L45)	No	Constant
CSIRO-Mk3.0	CSIRO (Australia)	T63 (L18)	No	–
CSIRO-Mk3.5	CSIRO (Australia)	T63 (L18)	–	–
ECHAM5/MPI-OM	MPI (GERMANY)	T63 (L31)	Yes	Constant
ECHO-G	MIUB, METRI, M&D (Germany/Korea)	T30 (L19)	–	Variable
FGOALS-g1.0	LASG/IAP (CHINA)	$2.8^{\circ}\times2.8^{\circ}$(L26)	Yes	Variable
GFDL-CM2.0	GFDL (USA)	$2.0^{\circ}\times2.5^{\circ}$(L24)	No	Variable
GFDL-CM2.1	GFDL (USA)	$2.0^{\circ}\times2.5^{\circ}$(L24)	Yes	Variable
GISS-AOM	NASA/GISS (USA)	$3^{\circ}\times4^{\circ}$(L12)	–	Constant
GISS-EH	NASA/GISS (USA)	$4^{\circ}\times5^{\circ}$(L20)	Yes	Variable
GISS-ER	NASA/GISS (USA)	$4^{\circ}\times5^{\circ}$(L20)	Yes	Variable
INGV-SXG	INGV (ITALY)	T106 (L19)	–	–
IPSL-CM4	IPSL(FRANCE)	$2.5^{\circ}\times3.75^{\circ}$(L19)	No	Constant
MIROC3.2(hires)	CCSR, NIES, FRCGC (JAPAN)	T106 (L56)	No	Variable
MIROC3.2(medres)	CCSR, NIES, FRCGC(JAPAN)	T42 (L20)	Yes	Variable
MRI-CGCM2.3.2	MRI (Japan)	T42 (L30)	No	Variable
PCM	NCAR (USA)	T42 (L26)	–	Variable
UKMO-HadCM3	HHCCPR/Met Office (UK)	$2.5^{\circ}\times3.75^{\circ}$(L19)	No	Constant
UKMO-HadGEM1	HHCCPR/Met Office (UK)	$1.25^{\circ}\times1.875^{\circ}$(L38)	No	Variable

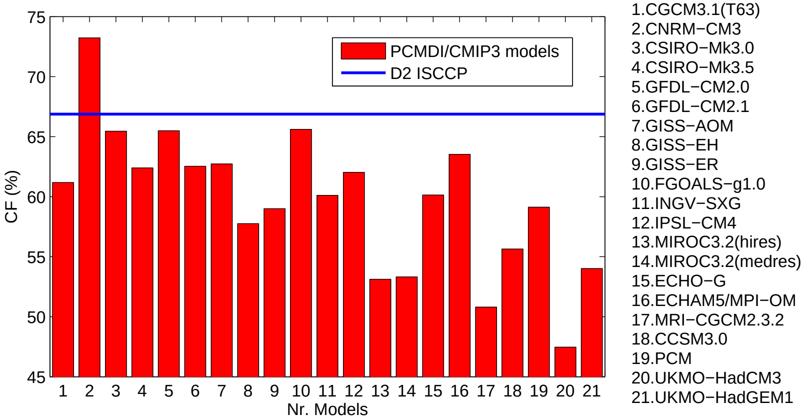

Fig. 1: Global mean of CF averaged over the period January 1984–December 1999.

ACPD
10, 21023–21046, 2010

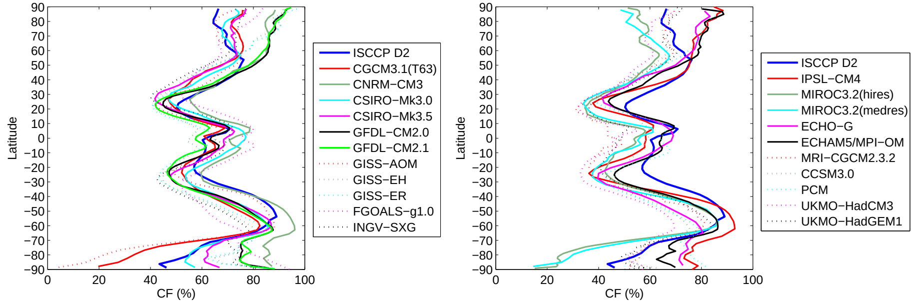

Fig. 2: CF zonal means of ISCCP and of PCMDI/CMIP3 models.

ACPD
10, 21023–21046, 2010

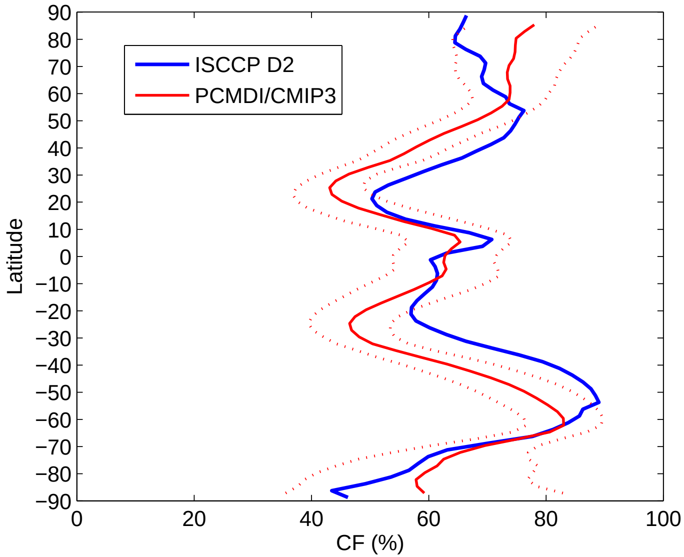

Fig. 3: CF zonal mean of ISCCP and of the *PCMDI/CMIP3 mean model*. The red dotted lines are one standard deviation CF zonal mean with respect to the mean model.

ACPD
10, 21023–21046, 2010

Cloud cover comparison

P. Probst et al.

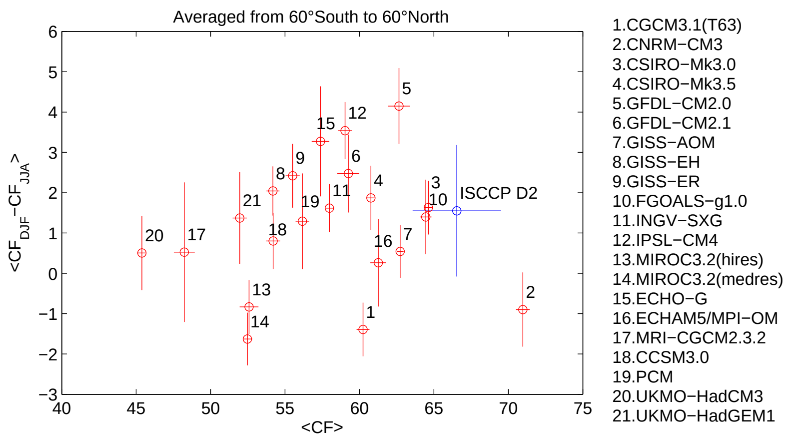

Fig. 4: CF comparison between the ISCCP D2 data (blue) and the PCMDI/CMIP3 models runs (red), both averaged from 60° South to 60° North. On the x-axis is the yearly average ($<CF>$), averaged over the whole time period, and the horizontal half-bar is twice the standard deviation with respect to $<CF>$; the y-axis is the average differences of CF for December, January and February (DJF) and June, July and August (JJA), and the vertical half-bar is twice the standard deviation of the amplitude $<CF_{DJF} - CF_{JJA}>$.

ACPD
10, 21023–21046, 2010

ACPD
10, 21023–21046, 2010

Cloud cover comparison

P. Probst et al.

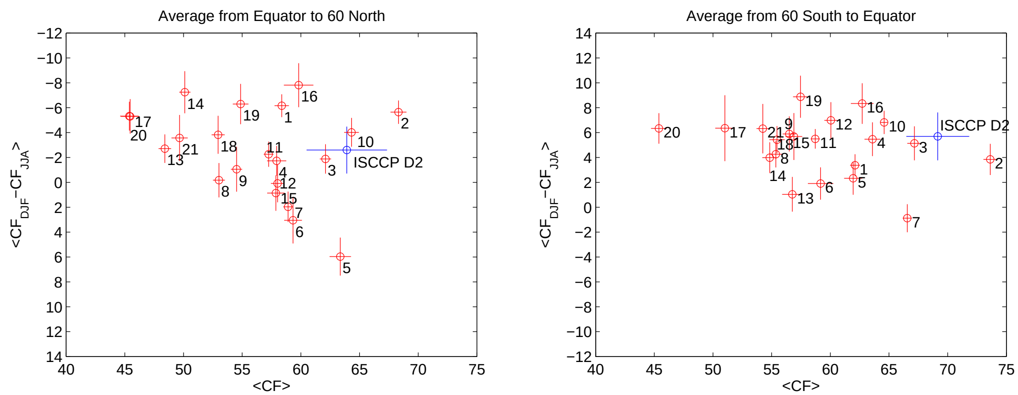

(a) Equator – 60° N

(b) 60° S – Equator

Fig. 5: Same as Fig. 4 but from Equator to 60° North for **(a)**, and from 60° South to Equator for **(b)**.

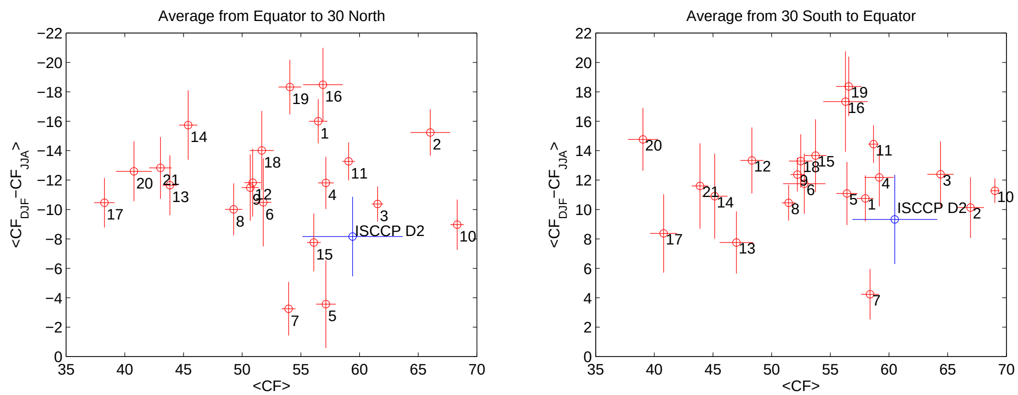

(a) Equator – 30° N

(b) 30° S – Equator

Fig. 6: The same of Fig. 4 but from Equator to 30° North for **(a)**, and from 30° South to Equator for **(b)**.

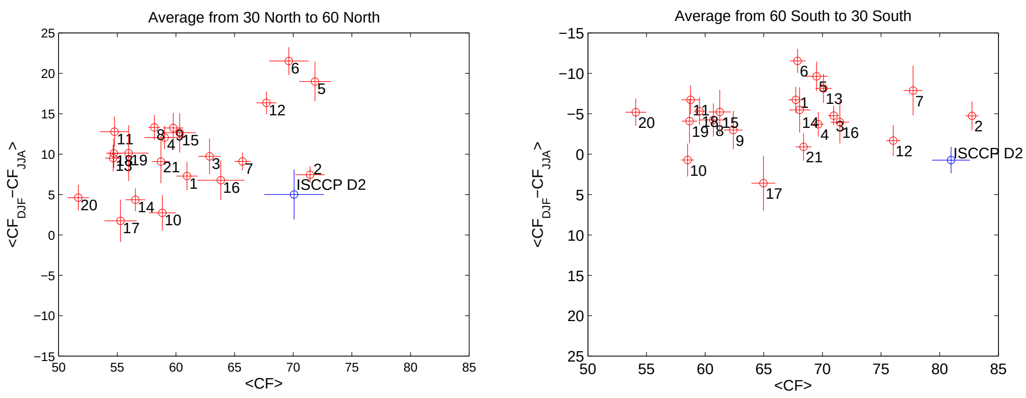

(a) 30° N - 60° N (b) 60° S – 30° S

Fig. 7: The same of Fig. 4 but from 30° North to 60° North for **(a)**, and from 60° South to 30° South for **(b)**.

ACPD
10, 21023–21046, 2010

Cloud cover comparison

P. Probst et al.